

Variability of the H₂O maser associated with the Mira variable RS Virginis

E. E. Lekht¹, J. E. Mendoza-Torres¹, G. M. Rudnitskij², and A. M. Tolmachev³

¹ Instituto Nacional de Astrofísica, Óptica y Electrónica, Luis Enrique Erro No. 1, Apdo Postal 51 y 216, 72840 Tonantzintla, Puebla, México

² Sternberg Astronomical Institute, 13 Universitetskij prospekt, Moscow 119899, Russia
e-mail: gmr@sai.msu.ru

³ Pushchino Radio Astronomy Observatory, Astrospace Center of the Lebedev Institute of Physics, Russian Academy of Sciences, Pushchino, Moscow Region 142290, Russia
e-mail: tolm@prao.psn.ru

Received 12 April 2001 / Accepted 2 July 2001

Abstract. The results of observations of the H₂O maser emission ($\lambda = 1.35$ cm) of the Mira-type variable star RS Vir are presented. The observations were carried out in 1981–2001 (JD = 2 444 900–2 451 995) on the RT-22 radio telescope of the Pushchino Radio Astronomy Observatory (Russia). The variability curve of the H₂O maser emission integrated flux $F_{\text{int}}(\text{H}_2\text{O})$ of RS Vir correlates with its visual light curve with some phase delay $\Delta\varphi = (0.05–0.35)P$ (P is the star’s period). The delay variations seem to be periodic at a timescale of 19–20 years (“superperiod” of the maser variations). If the variability of the H₂O maser RS Vir is caused by periodic action of pulsation-driven shock waves, the shock travel time from the photosphere to the inner boundary of the H₂O maser shell can be as long as $(3–5)P$. Another explanation is that maser variations may be connected with changing gas density in the masing region of the circumstellar envelope. In particular, long-term maser variations (the “superperiod”) may be caused by changing mass loss rate \dot{M} .

Key words. stars: variables: general – circumstellar matter – stars: individual: RS Vir – radio lines: stars – masers – shock waves

1. Introduction

At present, there are more than 300 known stellar sources of maser emission in the $6_{16}–5_{23}$ rotational line of H₂O at $\lambda = 1.35$ cm (Benson et al. 1990). The H₂O masers are localised in the inner layers of gas-dust circumstellar envelopes of variable red giants (Mira Ceti-type and semiregular stars with light cycles P of a few hundred days). Most circumstellar H₂O masers are variable, and their variations are tightly connected with the light variations of the central stars (see Berulis et al. 1998 and references therein).

From the point of view of long-term observations, it is of interest to compare the variability of a star in the H₂O line and in the optical range. Correlation between the variability curves in the H₂O line and at visual wavelengths, as well as accompanying changes in the H₂O line profile structure, reflect physical processes in the inner layers of

the red-giant circumstellar envelopes. Observations in the H₂O line offer a unique opportunity to study the region of acceleration of the material lost by the star: the inner radius of the H₂O maser zone around the star approximately coincides with radius R_c of dust condensation in circumstellar envelopes of late-type stars, and the main acceleration of gas begins precisely at R_c .

In red giants the H₂O line profile often contains two features: the main one close to the stellar velocity V_* , and another, fainter “blueshifted” feature, at a more negative velocity V_b , with $\Delta V = V_b - V_*$, as a rule, of about -1 to -5 km s⁻¹.

We report the results of monitoring of the M-type giant RS Vir (BD+05°2880a, HD 126753, IRC 00243, IRAS 14247+0454) in the H₂O $6_{16}–5_{23}$ line ($\lambda = 1.35$ cm), carried out from 1981 to 2001. RS Vir is one of the stellar objects we have been observing in the H₂O 1.35-cm maser line since early 1980s (Berulis et al. 1983). In our previous papers we have, in particular, traced in detail regularities in the H₂O variations for several late-type stars: RR Aql

Send offprint requests to: E. E. Lekht,
e-mail: lekht@inaoep.mx; mend@inaoep.mx

(Berulis et al. 1998), VX Sgr (Berulis et al. 1999), RT Vir (Lekht et al. 1999), R Leo (Esipov et al. 1999), W Hya (Rudnitskij et al. 1999), U Ori (Rudnitskij et al. 2000).

When compared with other programme stars, RS Vir is a relatively stable H₂O maser, which has been detectable throughout our monitoring interval since 1981. Other H₂O maser Miras of our sample that are similar in this respect to RS Vir are, e.g., U Ori, R Aql, RR Aql, U Her. A different kind of the stellar masers is represented by transient sources, appearing in the H₂O line above our detection threshold (~ 10 Jy) once per several stellar light cycles: R Leo, R Cas and U Aur (Esipov et al. 1999).

In the 4th Edition of the General Catalogue of Variable Stars (Kholopov et al. 1987) RS Vir is classified as a long-period variable of the Mira Ceti type. Its maximum amplitude in the visual is 7.0–14.6^m, limits of the spectral type variations are M6IIIe–M8e. GCVS lists for RS Vir the following light elements:

$$\text{Max} = \text{JD } 2\,445\,753 + 353^{\text{d}}.95 E. \quad (1)$$

More recently, the light elements of RS Vir were studied by Andronov et al. (1992), and they confirmed that elements (1) represent fairly well the light curve till early 1990s. However, Andronov et al. give slightly differing elements:

$$\text{Max} = \text{JD } 2\,439\,054.3 + 353^{\text{d}}.09 E. \quad (2)$$

We have checked (1) and (2) by plotting the data of the AFOEV visual observations of RS Vir for the interval of JD 2 440 000–2 451 905, retrieved from SIMBAD, as well as the visual data from Andronov et al. Figure 1 shows that indeed light elements (1) and (2) yield similar epochs of the maxima till present, i.e., the period of RS Vir has not significantly changed during the last 30 years.

The mean visual light curve of RS Vir, presented in Andronov et al. (1992), is strongly asymmetric, with the ascending branch noticeably steeper than the descending branch: $M - m = 0.37$. There is some hint to a bump on the ascending branch. These features of the light curve are indicative of strong shock effects in the atmosphere of the star (Vardya 1987, 1988).

The star RS Vir is a known source of maser emission, first detected in the lines of OH by Fillit et al. (1973), H₂O by Baudry & Welch (1974) and SiO by Spencer et al. (1981). RS Vir is also one of the stellar sources in which millimeter and submillimeter H₂O maser lines have been detected: $3_{13-2_{20}}$ at 183 GHz (González-Alfonso et al. 1998), $10_{29-9_{36}}$ at 321 GHz (Menten & Melnick 1991; Yates et al. 1995; Yates & Cohen 1996) and $5_{15-4_{22}}$ at 325 GHz (González-Alfonso et al. 1998; Yates et al. 1995; Yates & Cohen 1996). The presence of these H₂O lines in the spectrum of RS Vir testifies to a high excitation of the H₂O molecules in its circumstellar envelope.

The radial velocity of the star with respect to the local standard of rest (LSR), determined as the midpoint of the OH 1612-MHz line profile, is -14 km s⁻¹ (Te Lintel Hekkert et al. 1989).

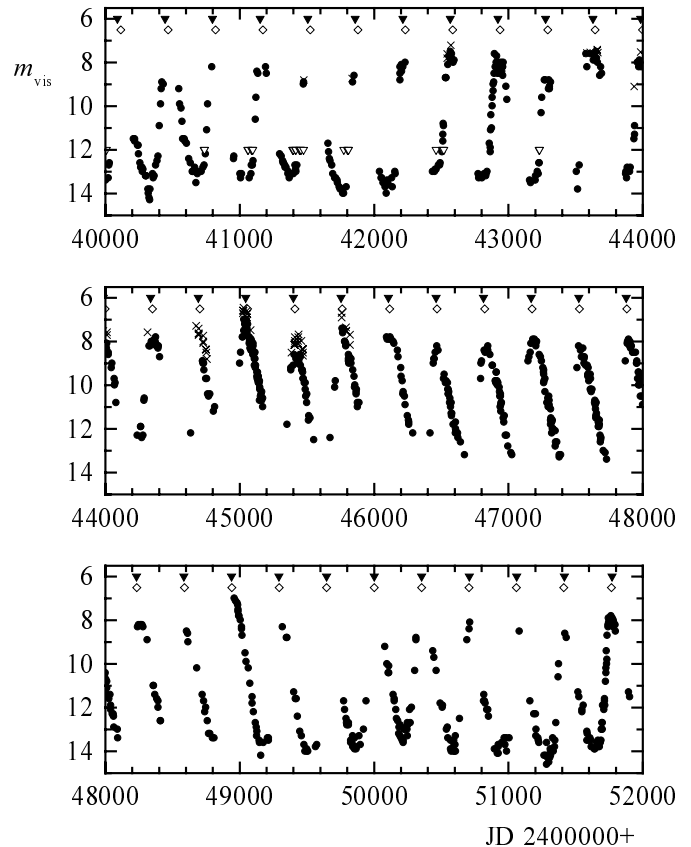


Fig. 1. Visual light curve of RS Vir (AFOEV data, circles), supplemented with data from Andronov et al. (1992) (crosses and, for upper limits, open triangles). The moments of visual maxima of the star are marked in the upper part of the panels; filled triangles: calculated with elements (1), diamonds: with elements (2).

Thermal emission in the CO line has not been detected (Nyman et al. 1992).

According to different authors, distance d to the star is 487 pc (Menten & Melnick 1991; Sivagnanam et al. 1988, 1989; Szymczak & Le Squeren 1999), 613 pc (Imai et al. 1997; González-Alfonso et al. 1998) or 642 pc (Spencer et al. 1981). In the majority of recent works the mean value $d = 600$ pc is taken. Thus, RS Vir is one of the most distant (and the strongest) stellar H₂O masers.

2. Observations

The observations were carried out on the 22-metre radio telescope RT-22 of the Radio Astronomy Observatory (Astrospace Centre of the Lebedev Institute of Physics, Russian Academy of Sciences) in Pushchino (Moscow Region). In 1981–1993 the receiving equipment included a 22-GHz maser amplifier, cooled by liquid helium, the system noise temperature T_N was 200–300 K, depending on the amplifier tuning and weather conditions. Since 1993 a cooled FET amplifier with $T_N = 150$ K was used. The receiver backend was a 128-channel filter-bank spectrometer, designed and made in the Sternberg Astronomical Institute, with a frequency

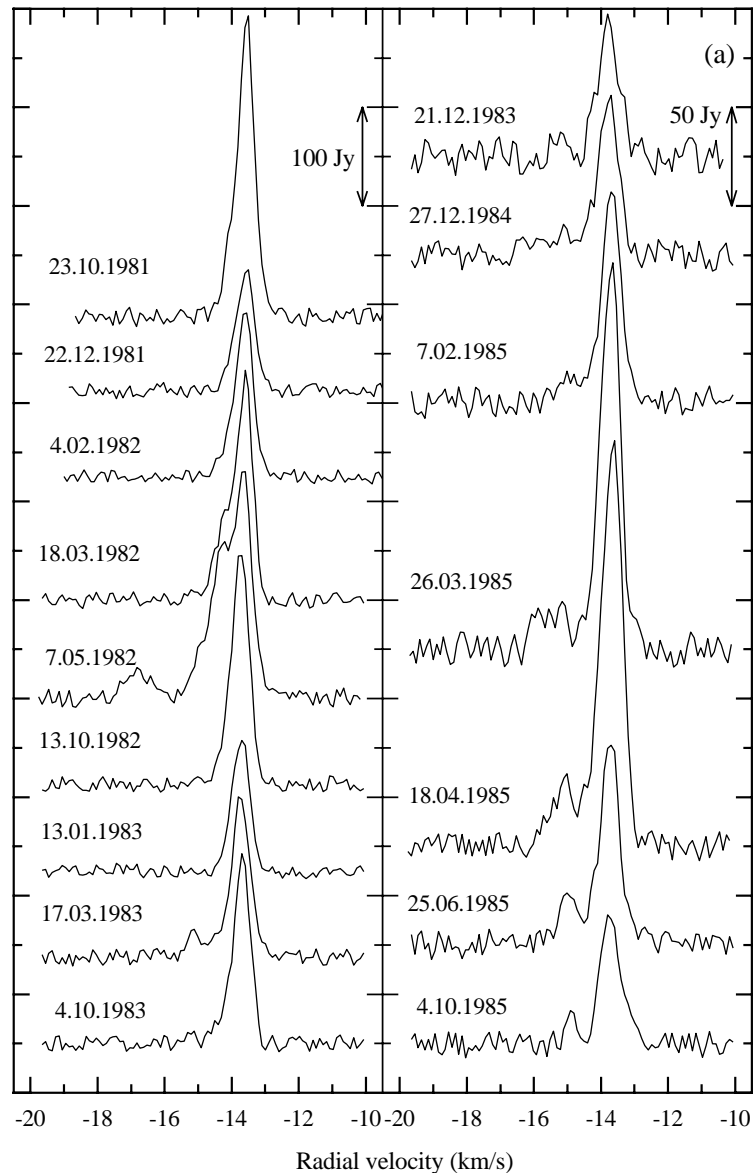


Fig. 2. Profiles of the H₂O maser emission line of the star RS Vir.

resolution of 7.5 kHz (0.101 km s^{-1} at the H₂O line frequency). Calibration was carried out by means of a gas-discharge noise tube, which in its turn was calibrated against noise signals of heated and cooled loads and by observations of Jupiter. The equipment and observational procedure were described in detail by Lekht et al. (1995, 1999).

The observed profiles of the H₂O line in RS Vir are presented in Figs. 2a–h. The vertical axis is the flux density F_ν in Janskys. The horizontal axis is the radial velocity relative to the Local Standard of Rest (V_{LSR} , km s^{-1}). The maximum V_{LSR} range covered by our observations is from -20 to -9 km s^{-1} .

For clearer presentation, all the profiles of Fig. 2 are given in Fig. 3 as a three-dimensional graph.

Figure 4a presents all the profiles of Fig. 2 plotted on the same graph, allowing us to get an idea of the persistent structure in the H₂O line profile of RS Vir. The main peak

is at $V_{\text{LSR}} \approx -14 \text{ km s}^{-1}$. In addition to it, a secondary peak is visible in Figs. 3 and 4 at $V_{\text{LSR}} \approx -16 \text{ km s}^{-1}$ (as in many profiles of Fig. 2, e.g., those of 1982 May 7, 1987 May 27, 1988 March 29, 1989 March 24, 1991 May, 1992 January–April, and others) as well as “blue” and “red” wings within $\pm 1 \text{ km s}^{-1}$ of the main peak (e.g., 1989 May 29). Figure 4b shows the H₂O profiles averaged over the decades of 1981–1991 and 1992–2001, as well as for the entire time interval of our observations. The velocity of the main peak, -14 km s^{-1} , is equal to the stellar velocity. At the same time, there are two “blueshifted” secondary features at -15 and -16 km s^{-1} ; they were probably present in the profile all the time. A small positive shift of the 1992–2001 mean profile with respect to that for 1981–1991 may be due to appearance of a feature in the positive velocity wing of the main peak. This feature is obvious in many profiles of Fig. 2, its peak flux density sometimes equalled that of the main peak and

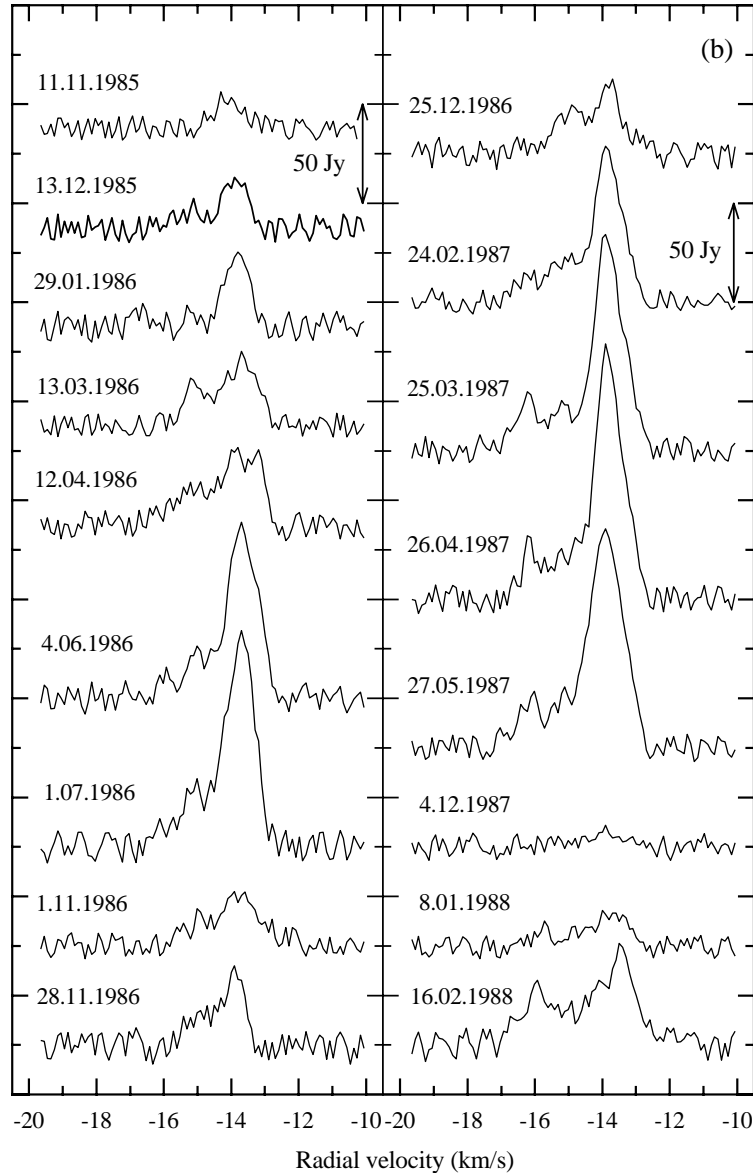


Fig. 2. continued.

shifted the mean weighted value of the radial velocity to about -13.5 km s^{-1} .

In Fig. 5a the integrated flux in the H₂O line is plotted vs. time. Figures 5b and c present the maximum flux density variations of the main peak at $V_{\text{LSR}} = -14 \text{ km s}^{-1}$ and of the secondary “blueshifted” feature at -16 km s^{-1} . The curve of Fig. 5c is fragmentary, because the “blueshifted” component was sometimes undetectable. It is visible that the integrated H₂O flux and both features vary nearly synchronously, though their intensities are probably not correlated.

For technical reasons (changes of the programme and of the equipment, etc.) there were some interruptions in the series of the observations: about one year in 1983–1984 and in 1993–1994, five months in 2000–2001. Nevertheless, the overall pattern of the long-term maser variability is obvious. The $F(\text{H}_2\text{O})$ curve follows the light curve of the

star, the H₂O maxima lag behind the visual maxima by $\Delta\varphi = 0.05\text{--}0.35$ (Fig. 6). There is a systematic trend in the phase delay: since the beginning of our observations, in 1982–1991, the value of $\Delta\varphi$ was on the average increasing from 0.16 to 0.27, with an outburst to 0.35 at the beginning of 1986. Since 1991 till 1997 $\Delta\varphi$ decreased to 0.05, and then again slightly increased to 0.12–0.14 for the last two maxima (probably marking the beginning of the next activity cycle). We discuss possible causes of this trend in the next section.

3. Model of variability of the circumstellar H₂O maser RS Vir

The star RS Vir has been repeatedly studied in the 22-GHz H₂O line by Baudry & Welch (1974), Lépine et al. (1974, 1978), Hagen (1979), Crocker & Hagen (1983).

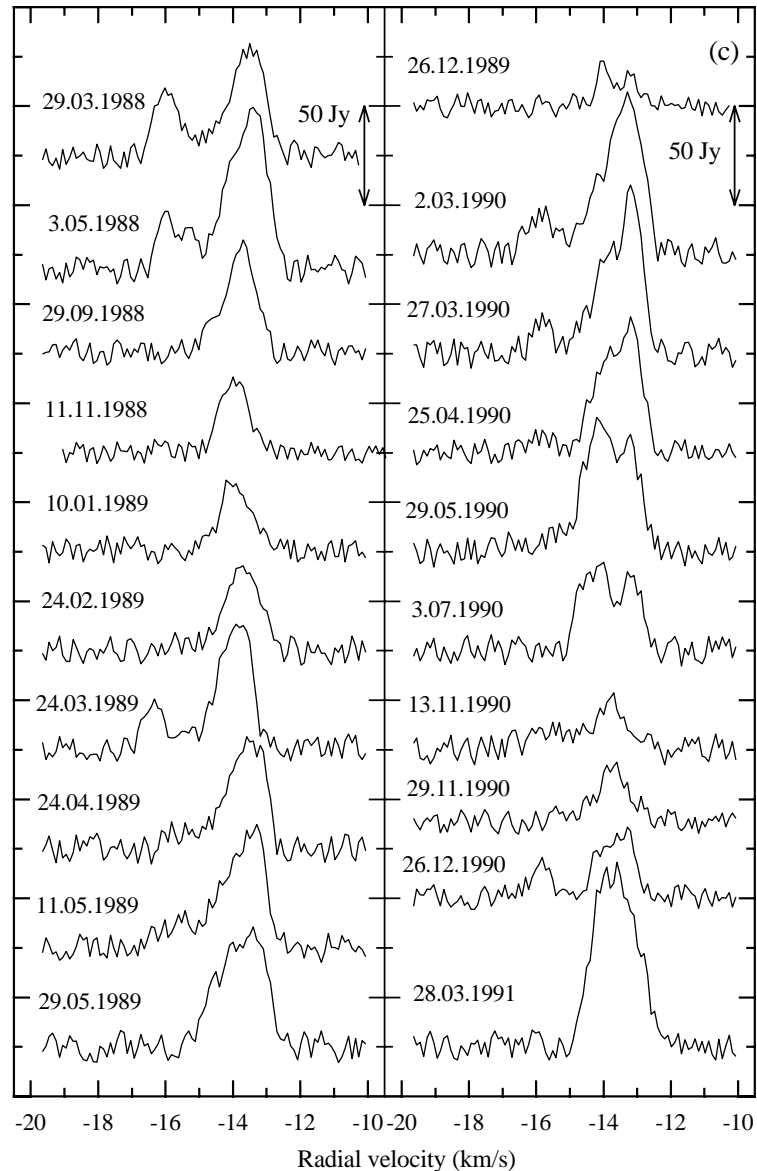


Fig. 2. continued.

The most detailed study of the H₂O variability was undertaken by Cox & Parker (1979) in 1974–1977 (JD 2442350–2443300). Their observations covered two light cycles of RS Vir. Cox & Parker also noted some correlation of the H₂O data with the visual brightness. However, the phase difference between the H₂O and visual maxima is large, about $0.7P$.

In later years, RS Vir was observed in the 1.35-cm H₂O line by Barvainis & Deguchi (1989), Comoretto et al. (1990), Menten & Melnick (1991), Palagi et al. (1993), Takaba et al. (1994), Szymczak & Le Squeren (1999). The profiles of the H₂O line, obtained in these works at epochs close to our observations (if available), are in general consistent with our results.

The observed correlation between the visual brightness of the star and H₂O maser emission flux (Fig. 5) can be explained by three possible mechanisms: (1) periodic

heating of circumstellar dust grains (and, as a consequence, of the surrounding gas) by variable IR emission of the star (Gómez Balboa & Lépine 1986); (2) action of shock waves driven by stellar pulsation on the region of maser generation (Rudnitskij & Chuprikov 1990; Berulis et al. 1998); (3) variations in density associated with variations in mass loss rate \dot{M} (Elitzur 1992).

Mechanism (1) results in small, constant phase delays $\Delta\varphi$ of variations of $F_{\text{int}}(\text{H}_2\text{O})$ relative to the visual light curve; this is frequently observed in the H₂O masers associated with Mira variables (Berulis et al. 1998). However, we consider models (2) and (3) to be more realistic. We accept that the H₂O masering region is localised in a quasi-stationary layer (QSL) of gas and dust at $R \sim 10^{14}$ cm. QSL is visible in the IR vibrational lines of CO in many Miras (Hinkle et al. 1984).

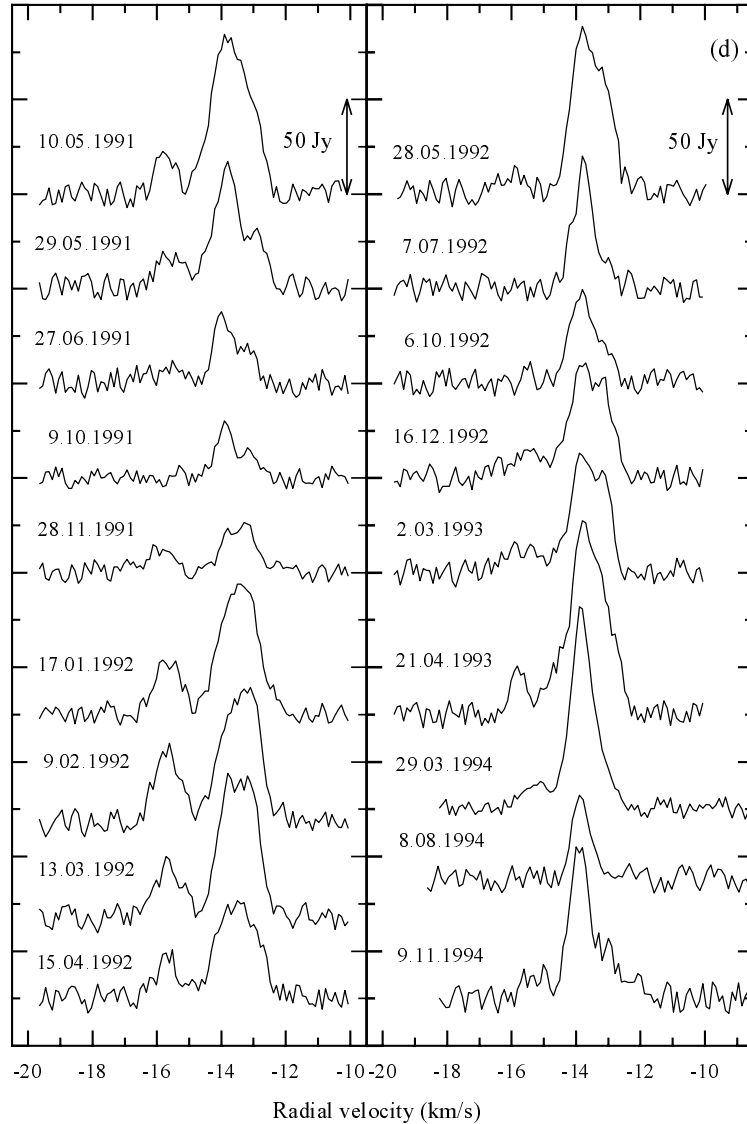


Fig. 2. continued.

3.1. Shock excitation of the maser

In model (2) the H₂O maser in QSL is directly affected by weak shocks with $v_s \sim 5\text{--}10\text{ km s}^{-1}$, driven by stellar pulsations (Rudnitskij & Chuprikov 1990). The action of the shock consists of density enhancement and an almost prompt heating of gas, whereas dust remains for a while cooler than the gas; thus, a nonequilibrium state, necessary for the maser pumping, is supported in the postshock zone.

The kinematics of the H₂O maser profiles is explained in shock model (2) as follows. The main peak at V_* appears in the limb part of the H₂O masering shell. The “blueshifted” peak at V_b comes from the approaching side of the shell, and the “redshifted” peak, from the receding side (partly blocked by the star). The velocity difference in RS Vir, $V_b - V_* \approx -2\text{ km s}^{-1}$, may be too low for a shock: the velocity of sound in the inner parts of the circumstellar envelope ($T \sim 1000\text{ K}$) is at least 3 km s^{-1} , and shock

velocity $v_s \sim 5\text{--}10\text{ km s}^{-1}$. We suppose that the peaks at -15 and -16 km s^{-1} originate at lower line-of-sight velocities in the regions closer to the limb, where maser amplifications paths are longer. Probably, features at velocities more negative than -16 km s^{-1} (coming from the star’s line of sight) were also present, but remained below our detection limit ($\sim 10\text{ Jy}$).

If several weak shocks are simultaneously propagating through QSL, the “blueshifted” feature can be attributed to the “younger” (and faster) shock; then, it should brighten earlier than the main peak. However, the synchronous variation of the fluxes in Figs. 5b and c does not support this.

Cox & Parker (1979) also plotted the integral, main-peak and “blueshifted”-feature (at -15.6 km s^{-1} in their data) fluxes separately. They too note that the main peak and the “blueshifted” feature were changing synchronously, though the main-peak brightening

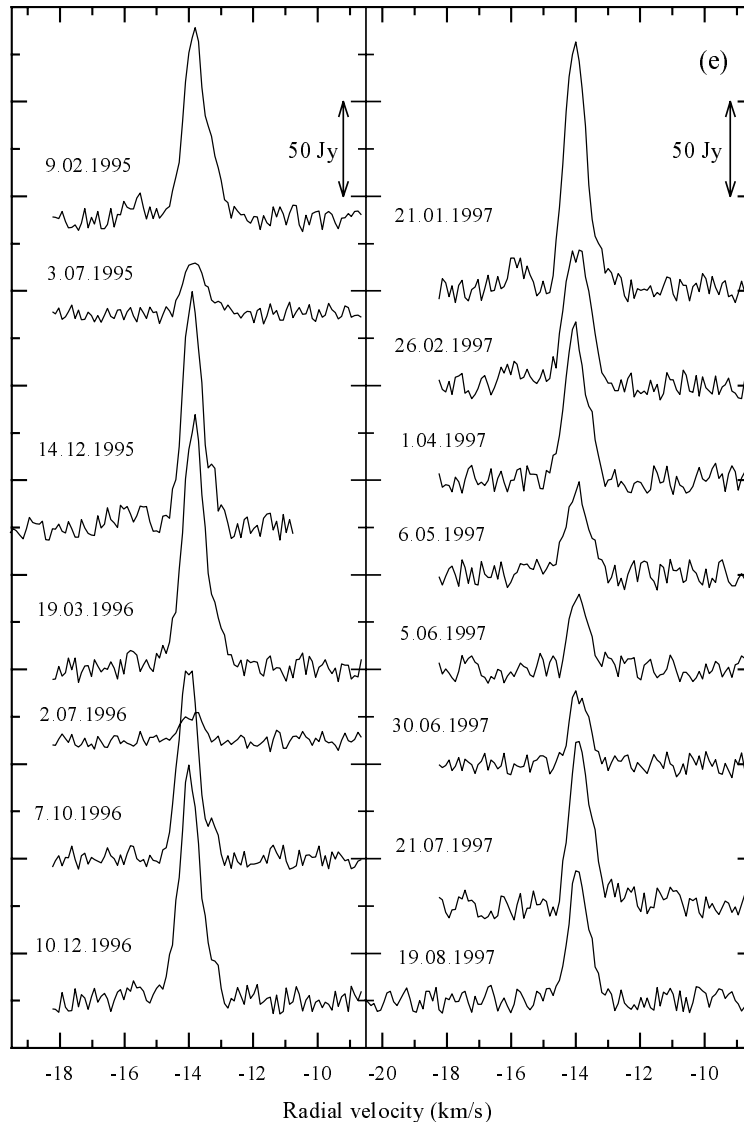


Fig. 2. continued.

at JD 2443300 was not accompanied by a flare of the “blueshifted” component.

In model (2) the true time delay can be $\Delta t = (\Delta\varphi + n)P$, i.e., should be incremented by an integer number of the stellar light periods. Then, Δt is the travel time of the shock, connected with the visual maximum of a star, from the photosphere to the H₂O maser layer in the circumstellar envelope.

The time behaviour of $\Delta\varphi$ indicates that an increase of $F_{\text{int}}(\text{H}_2\text{O})$ may be connected to one of the previous visual maxima, not with the latest one. A shock wave with velocity $v_s \lesssim 10 \text{ km s}^{-1}$ does not spend energy in ionisation of hydrogen and can propagate to rather large distances from the stellar surface, because its radiative losses are quite minor. The main shock’s energy losses are due to the emission of heated dust behind the shock front and with dissociation and/or excitation of molecular hydrogen (if H₂ is present in the circumstellar medium in a noticeable amount) (Rudnitskij 1997). To find the actual

propagation time of the shock to the H₂O masering region ($R \sim (1-2) \times 10^{14} \text{ cm}$), a cross-correlation analysis of the star’s light curves in the visual and in the H₂O line is required.

We have constructed normalised cross-correlation function (Fig. 7) between the time dependence of $F(\text{H}_2\text{O})$ and visual light curve:

$$R(\tau) = \langle F_{\text{H}_2\text{O}}(t + \tau) F_{\text{vis}}(t) \rangle / \langle F_{\text{H}_2\text{O}}(t + \tau) F_{\text{vis}}(t) \rangle_{\text{max}}. \quad (3)$$

Here τ is the time delay between the light curve and maser variation. As the flux in the visual we have used the value

$$F_{\text{vis}} = 2.512^{14 - m_{\text{vis}}}, \quad (4)$$

in arbitrary units, referred to the light minimum magnitude of 14^m. We used 100 points of $F(\text{H}_2\text{O})$ and 780 points of F_{vis} . This yielded 119 points of $R(\tau)$ on an interval of $\tau = 0-3540^{\text{d}}$ ($0-10P$). The data are incomplete: in addition to the above-mentioned gaps in the $F(\text{H}_2\text{O})$ time

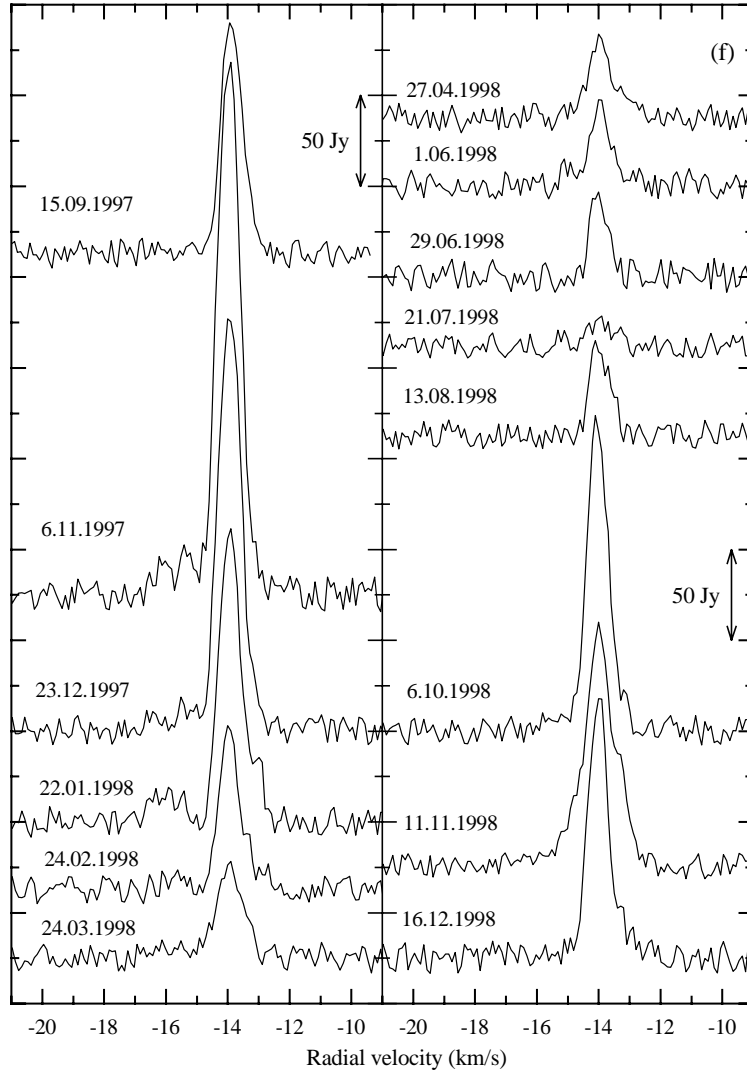


Fig. 2. continued.

series, the visual maxima of RS Vir were unobservable in 1994–1996 because of proximity of the star to the Sun.

Nevertheless, the $R(\tau)$ curve seems to be rather instructive. There is a small plateau from $\tau = 0$ to 90° [$\Delta\varphi = (0-0.25)P$], reflecting the prompt connection between the maser maximum and light maximum. The periodicity of $R(\tau)$ is obvious. An interesting feature of the $R(\tau)$ curve is that, after two lower-amplitude maxima at $\tau = 1P$ and $2P$, the next peaks, reaching almost unity, are located at $\tau = 3, 4$ and $5P$; the amplitudes of the successive peaks are again lower. If we associate the shock strength (characterised by the value of the shock velocity, v_s) with the height of the corresponding light maximum, then the above correlation indicates a possible effect on the H₂O maser of the light maxima that took place 3, 4, 5 stellar periods before. This is consistent with the time necessary for a shock leaving the stellar photosphere with, say, $v_{s0} \sim 10 \text{ km s}^{-1}$ to reach the maser generation layer

out at $R_c \sim 10^{14} \text{ cm}$. If shock velocity v_s is decreasing with distance as

$$v_s = v_{s0} \left(\frac{R_{\text{ph}}}{R} \right)^\alpha, \quad (5)$$

where $\alpha \sim 1$ (Willson 1976), then time required to reach the inner QSL boundary (R_c) is

$$\Delta t = \frac{R_c^2 - R_{\text{ph}}^2}{2v_{s0}R_{\text{ph}}}, \quad (6)$$

and indeed, with $v_{s0} = 10 \text{ km s}^{-1}$, $R_{\text{ph}} = 3 \times 10^{13} \text{ cm}$, $R_c = 10^{14} \text{ cm}$, the shock travel time is ~ 5 years.

During our study, the delay of the $F(\text{H}_2\text{O})$ variations with respect to the visual light curve $\Delta\varphi$ (Fig. 6) was varying in the limits of $0.05-0.35P$. The long-term behaviour of $\Delta\varphi$ can be described by an almost complete sine wave with a period of 19–20 years. This value can be considered as a “superperiod” in the stellar maser variability. Earlier we detected such a “superperiod” of 9 years in the H₂O maser variations of the Mira U Ori

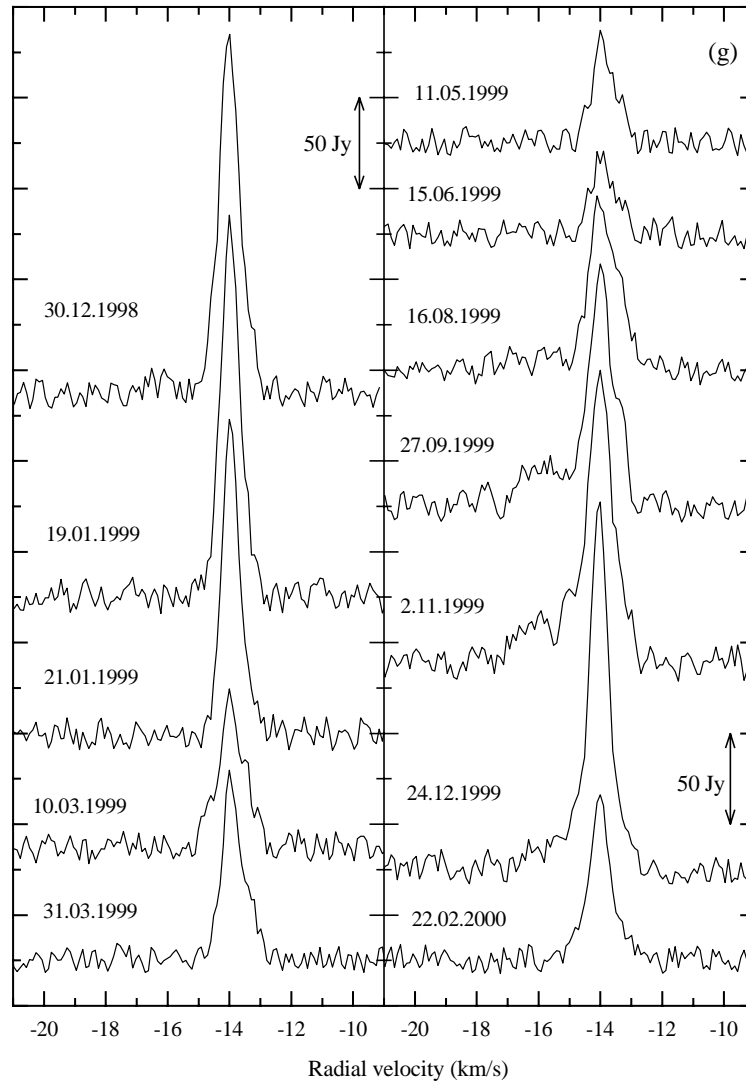


Fig. 2. continued.

(Berulis et al. 1994). Thus, time delay $\Delta t = (\Delta\varphi + n)P$, where $n = 3-5$, is changing in a quasi-periodic manner both in U Ori and RS Vir. As a possible cause of this effect, Rudnitskij et al. (2000) have proposed the changing distance of the QSL inner boundary, R_c , from the stellar photosphere. This results in varying time delay Δt . The “superperiod” may be due to stronger shocks arising once in a few stellar light cycles.

In this connection, we note the higher maxima in the light curve of Fig. 1: JD 2442 567, $E = -9$ in the light elements (1), $m_{\text{vis}} = 7.5$; 2445 045, $E = -2$, $m_{\text{vis}} = 7.0$; 2448 939, $E = 9$, $m_{\text{vis}} = 7.0$; and, most recently, 2451 770, $E = 17$, $m_{\text{vis}} = 7.8$. In the model considered the high H₂O flux peak after the light maximum JD 2450 708 is actually connected with the light maximum JD 2448 939, five cycles earlier. The H₂O peak after JD 2445 045 is due to the high visual maximum at JD 2442 567, also preceding by $5P$. As for the H₂O peak at JD 2451 416, the corresponding light maxima that took place 3, 4, $5P$ before have no visual data: as noted above, in these years the

star was unobservable near its light maximum. The time difference between the H₂O maser bursts at JD 2451 416 and 2445 045 is 18 years, very close to the “superperiod” of 19–20 years, traced above in the variations of $\Delta\varphi$. The shortest delays were observed near the edges of our observational interval, in 1982 and 2000, again suggesting that higher light maxima generate faster shocks.

As for the H₂O outburst of RS Vir near JD 2443 300, observed by Cox & Parker (1979), it is difficult to trace its history in the previous visual light curve. The brightness curve given by Cox & Parker covers only the preceding two light cycles, while the curve of our Fig. 1 again poorly samples the preceding light maxima, because of the star’s proximity to the Sun. Thus, nothing can be said with certainty about the origin of the H₂O peak at JD 2443 300.

According to Wood (1979), when propagating through QSL outward from the star, subsequent faster shocks (generated in a higher visual maximum) can overtake the slower preceding ones and merge with them, thus enhancing the effect on the maser. A similar mechanism was

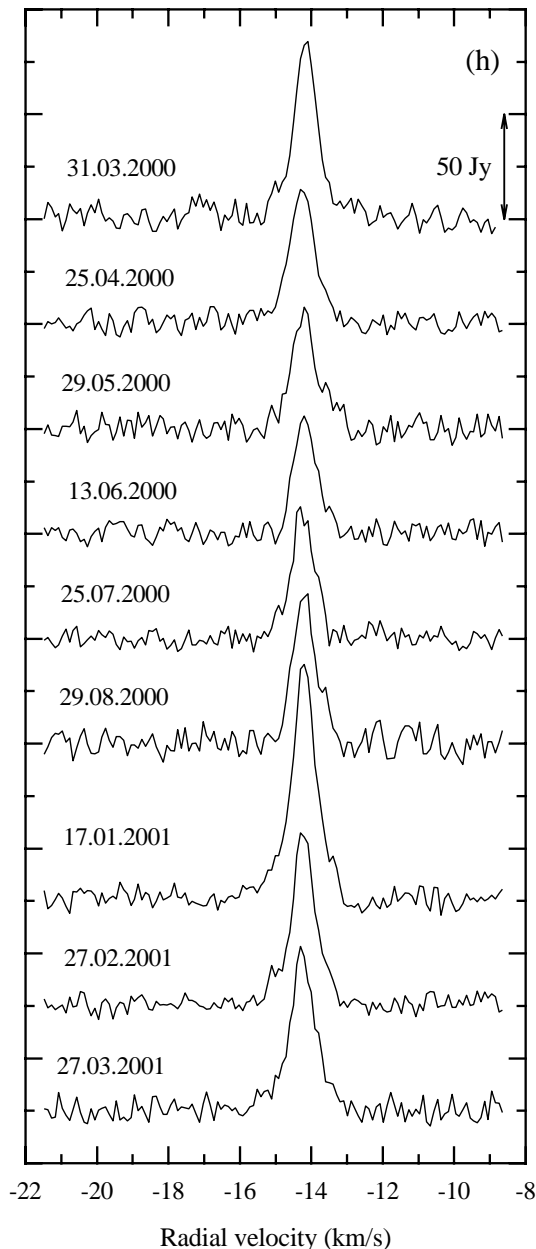


Fig. 2. continued.

proposed by Gómez Balboa & Lépine (1986) to explain the superperiod in the H₂O maser associated with the semiregular variable W Hya. This effect may account for the more powerful H₂O maser outbursts, seen in RS Vir by Cox & Parker (1979) and by us (Fig. 5).

3.2. The effect of mass loss rate variations

While not excluding the possibility of periodic shock impact as the cause of the H₂O maser variations, model (3) with short-term variations of mass loss rate \dot{M} (through the stellar light cycle P) may yield similar effects on the circumstellar gas density and, accordingly, on the maser pumping rate. Longer-term variations of \dot{M} also affect the radial position of the masering zone as $R_c = \dot{M}^{2/3}v^{-1}$,

where v is the shell expansion velocity (Elitzur 1992). The masering zone moves in and out with changing \dot{M} . This readily accounts for the variations of time delay $\Delta\varphi$ between the light curves in the visual and in the H₂O line.

In model (3) the short-term mass loss changes affect the entire maser zone simultaneously, and thus the variations of the maser at the approaching, limb and receding parts of the shell should be synchronous, as suggested by our Fig. 5 and by the data of Cox & Parker (1979).

To test this hypothesis further, it would be of interest to monitor \dot{M} by CO-line or IR observations. However, the \dot{M} data on RS Vir are almost totally lacking, since this star has not been detected in thermal CO emission, see above. The only value of \dot{M} found in the literature comes from a theoretical estimate of Ivezić & Elitzur (1995), who,

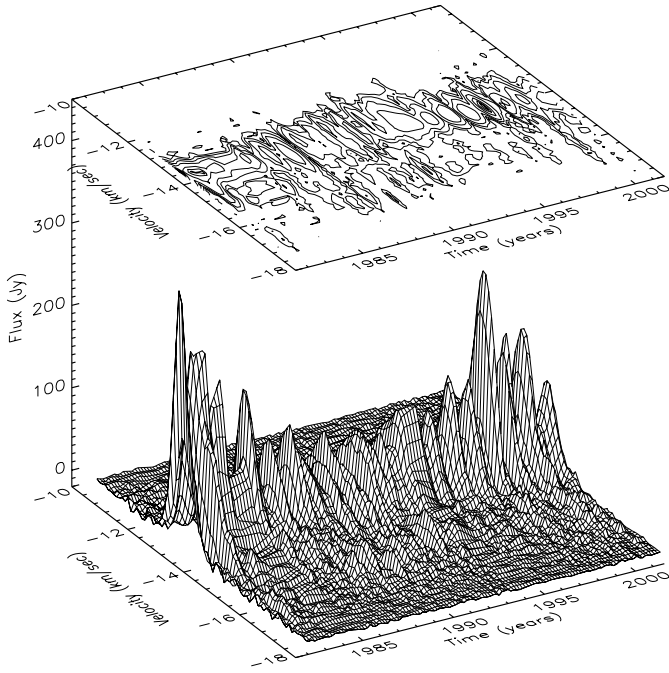


Fig. 3. Three-dimensional presentation of the H₂O line profiles of RS Vir.

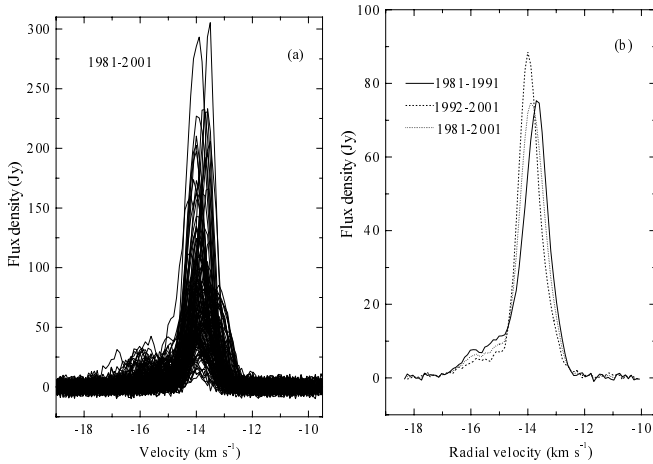


Fig. 4. Overlay of all the H₂O line profiles of RS Vir **a)**; averaged profiles for the first and second decades and for the entire monitoring interval **b)**.

based on the IRAS data, estimated the mass loss rate for RS Vir to be $1.0 \times 10^{-6} M_{\odot} \text{yr}^{-1}$. So far, this isolated estimate cannot be used to study \dot{M} variations, although it confirms the rather high \dot{M} ranking of RS Vir among circumstellar H₂O masers: the weakest H₂O masers have $\dot{M} \sim 10^{-7} M_{\odot} \text{yr}^{-1}$, i.e., by an order of magnitude lower (Elitzur 1992).

4. Conclusion

In this work we have presented the profiles of the H₂O 1.35-cm emission line of the M-giant RS Vir for 1981–2001. The variability of the H₂O maser RS Vir correlates with the visual light curve of the star. However, phase delay $\Delta\varphi$

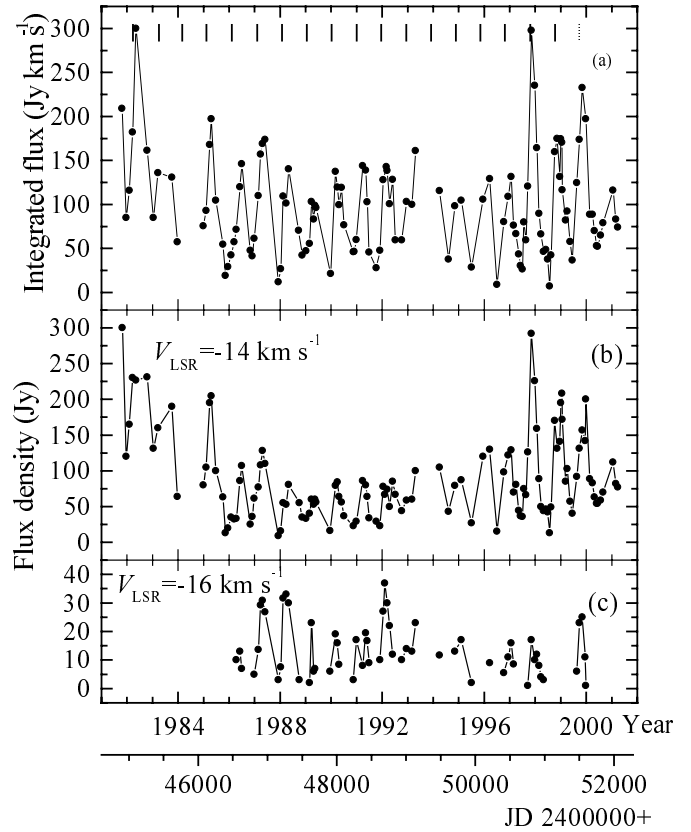


Fig. 5. Time dependence of the integrated H₂O maser flux of RS Vir **a)**. Vertical bars at the top denote the epochs of light maxima, calculated with elements (1). Variations of the peak flux density at $V_{\text{LSR}} = -14 \text{ km s}^{-1}$ **b)** and -16 km s^{-1} **c)**.

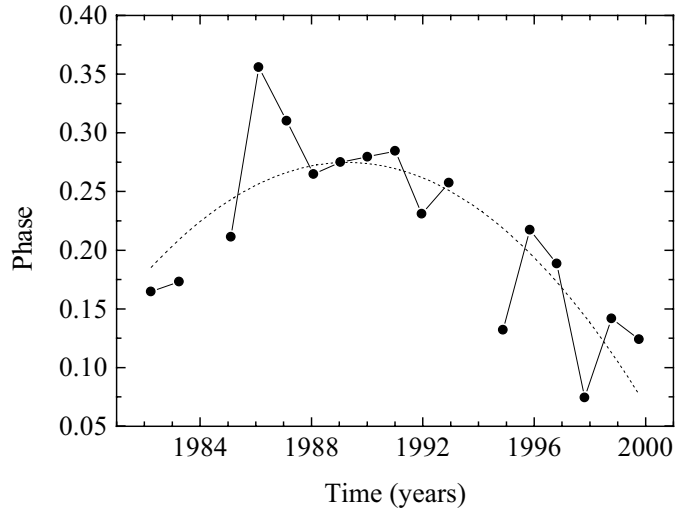


Fig. 6. Phase delay of the H₂O maser variations relative to the visual light curve.

of the $F_{\text{int}}(\text{H}_2\text{O})$ variations with respect to the optical pulsations varied during our observations between 0.35 and 0.05 P . If the variability of the H₂O maser RS Vir is caused by periodic pumping action of pulsation-driven shock waves, the travel time of the shocks from the photosphere to R_c , the inner boundary of the H₂O maser region, may be as long as $(3-5)P$. Alternatively, the maser

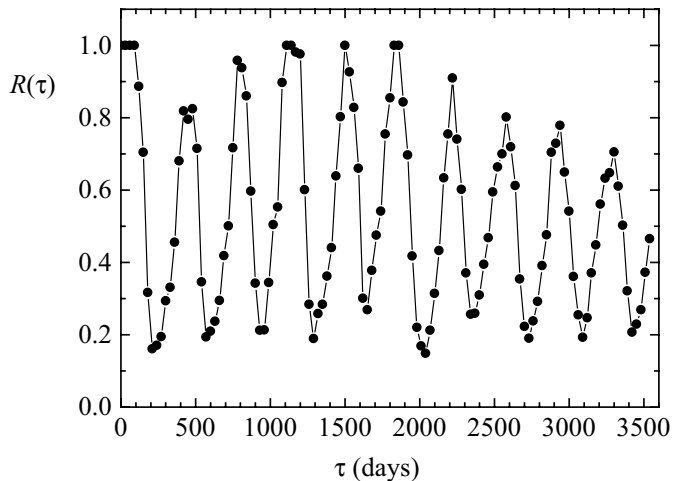


Fig. 7. Cross-correlation function between the H₂O maser variations and visual light curve.

variations may be connected to changing gas density in the masering region of the circumstellar envelope, caused by varying mass loss rate \dot{M} . In particular, long-term maser variations – the “superperiod” – also may be caused by changing \dot{M} .

A conclusive test of the models could be VLBI mapping of the star at several epochs. In case of shock excitation, VLBI can trace propagation of shocks in the masering QSL as outward proper motions of the H₂O emission features. With variable mass loss rate, the position of the masering zone should move in and out on the timescale of the $\Delta\varphi$ variation superperiod, 19–20 years. Unfortunately, RS Vir has never been mapped in the H₂O line. The only attempt, made in June 1994 and January 1995 (Imai et al. 1997), was unsuccessful; the star was not detected. For model (3), simultaneous interferometric monitoring of the IR stellar diameter can be useful. For instance, Tuthill et al. (1995) reported an almost twofold increase of the interferometric size of *o* Cet, measured at $\lambda = 2.2 \mu\text{m}$, over one and a half year, between July 1992 and December 1993. This may imply an episode of increased mass loss rate \dot{M} and a build-up of a denser-than-usual zone in the circumstellar envelope. Such an enhancement of density also can increase the maser intensity.

Acknowledgements. We thank the staff of the Pushchino Radio Astronomy Observatory for the great help with the H₂O observations. The work was supported by the Russian Program of Integration of Science and Higher School (project AO 107). The RT-22 telescope is supported by the Ministry of Industry, Science and Technology of the Russian Federation, facility registration number 01–10. This research made use of the AFOEV visual observations from the SIMBAD database, operated at Centre des données astronomiques de Strasbourg (France). We

are grateful to the referee, Dr. E. Seaquist, whose comments helped to improve the article.

References

- Andronov, I. L., Kudashkina, L. S., & Romanenko, T. V. 1992, *Peremennye Zvezdy*, 23, 23
- Barvainis, R., & Deguchi, S. 1989, *AJ*, 97, 1089
- Baudry, A., & Welch, W. J. 1974, *A&A*, 31, 471
- Benson, P. J., Little-Marenin, I. R., Woods, T. C., et al. 1990, *ApJS*, 74, 911
- Berulis, I. I., Lekht, E. E., Pashchenko, M. I., & Rudnitskij, G. M. 1983, *SvA*, 27, 179
- Berulis, I. I., Lekht, E. E., & Pashchenko, M. I. 1994, *Astron. Lett.*, 20, 115
- Berulis, I. I., Lekht, E. E., Munitsyn, V. A., & Rudnitskij, G. M. 1998, *Astron. Repts.*, 42, 346
- Berulis, I. I., Pashchenko, M. I., & Rudnitskij, G. M. 1999, *Astron. Astrophys. Trans.*, 18, 77
- Comoretto, G., Palagi, F., Cesaroni, R., et al. 1990, *A&AS*, 84, 179
- Cox, G. G., & Parker, E. A. 1979, *MNRAS*, 186, 197
- Crocker, D. A., & Hagen, W. 1983, *A&AS*, 54, 405
- Elitzur, M. 1992, *Astronomical Masers* (Dordrecht: Kluwer), 265
- Esipov, V. F., Pashchenko, M. I., Rudnitskij, G. M., et al. 1999, in *Asymptotic Giant Branch Stars*, Proc. 191st Symp. IAU, ed. T. Le Bertre, A. Lèbre, & C. Waelkens (San Francisco: ASP), 201
- Fillit, R., Foy, R., & Gheudin, M. 1973, *ApL*, 14, 135
- Gómez Balboa, A. M., & Lépine, J. R. D. 1986, *A&A*, 159, 166
- González-Alfonso, E., Cernicharo, J., Alcolea, J., & Orlandi, M. A. 1998, *A&A*, 334, 1016
- Hagen, W. 1979, *PASP*, 91, 165
- Hinkle, K. H., Scharlach, W. W. G., & Hall, D. N. B. 1984, *ApJS*, 56, 1
- Imai, H., Sasao, T., Kameya, O., et al. 1997, *A&A*, 317, L67
- Ivezić, Ž., & Elitzur, M. 1995, *ApJ*, 445, 415
- Kholopov, P. N., Samus', N. N., Goranskii, V. P., et al. 1987, *General Catalogue of Variable Stars*, 4th ed., vol. III (Moscow: Nauka), 298
- Lekht, E. E., Mendoza-Torres, J. E., & Sorochenko, R. L. 1995, *ApJ*, 443, 222
- Lekht, E. E., Mendoza-Torres, J. E., Pashchenko, M. I., & Berulis, I. I. 1999, *A&A*, 343, 241
- Lépine, J. R. D., Paes de Barros, M. H., & Gammon, R. H. 1976, *A&A*, 48, 269
- Lépine, J. R. D., Le Squeren, A. M., & Scalise, E. 1978, *ApJ*, 225, 869
- Menten, K. M., & Melnick, G. J. 1991, *ApJ*, 377, 647
- Nyman, L.-Å., Booth, R. S., Carlström, U., et al. 1992, *A&AS*, 93, 121
- Palagi, F., Cesaroni, R., Comoretto, G., et al. 1993, *A&AS*, 101, 153
- Rudnitskij, G. M. 1997, *Ap&SS*, 251, 259
- Rudnitskij, G. M., & Chuprikov, A. A. 1990, *SvA*, 34, 147
- Rudnitskij, G. M., Lekht, E. E., & Berulis, I. I. 1999, *Astron. Lett.*, 25, 467
- Rudnitskij, G. M., Lekht, E. E., Mendoza-Torres, J. E., et al. 2000, *A&AS*, 146, 385
- Sivagnanam, P., Le Squeren, A. M., & Foy, F. 1988, *A&A*, 206, 285

- Sivagnanam, P., Le Squeren, A. M., Foy, F., & Tran Minh, F. 1989, *A&A*, 211, 341
- Spencer, J. H., Winnberg, A., Olmon, F. M., et al. 1981, *AJ*, 86, 392
- Szymczak, M., & Le Squeren, A. M. 1999, *MNRAS*, 304, 415
- Takaba, H., Ukita, N., Miyaji, T., & Miyoshi, M. 1994, *PASJ*, 46, 629
- te Lintel Hekkert, P., Versteeg-Hansel, H. A., Habing, H. J., & Wiertz, M. 1989, *A&AS*, 78, 399
- Tuthill, P. G., Haniff, C. A., & Baldwin, J. E. 1995, *MNRAS*, 277, 1541
- Vardya, M. S. 1987, *A&A*, 182, 75
- Vardya, M. S. 1988, *A&AS*, 73, 181
- Willson, L. A. 1976, *ApJ*, 205, 172
- Wood, P. R. 1979, *ApJ*, 227, 220
- Yates, J. A., & Cohen, R. J. 1996, *MNRAS*, 278, 655
- Yates, J. A., Cohen, R. J., & Hills, R. E. 1995, *MNRAS*, 273, 529